Electron-impact ionization of Ne($2p$) and Ar($3p$) at intermediate energies: Role of the postcollision interaction

Xiaoqing Hu,[1,2,*] Cong-Zhang Gao,[2] Zhanbin Chen,[3,4] Jianguo Wang,[2] Yong Wu,[2,†] and Yang Wang[1,‡]

[1]*Academy of Fundamental and Interdisciplinary Sciences, Harbin Institute of Technology, Harbin 150080, People's Republic of China*

[2]*Institute of Applied Physics and Computational Mathematics, Beijing 100088, China*

[3]*School of Science, Hunan University of Technology, Zhuzhou 412007, China*

[4]*College of Science, National University of Defense Technology, Changsha 410073, China*

(Received 29 September 2017; published 3 November 2017; publisher error corrected 30 November 2017)

We present the absolute triple differential cross section (TDCS) for single ionization of Ne($2p$) at an impact energy of 599.6 eV and Ar($3p$) at 195 eV. The role of the postcollision interaction (PCI) is studied using a high-order distorted-wave Born approximation model with a continuum distorted-waves expansion. Both the second- and third-order effects are considered in the present calculations, and the third-order distorted wave Born approximation model is reported in the (e,$2e$) reaction. The calculated results show satisfactory agreement with experimental data. The magnitude of the absolute TDCS is enhanced by a factor 2–3 when the strength factor γ of the PCI amplitude is summarized just from 0 to 2. This proves that the PCI plays an important role in the absolute TDCS of the (e,$2e$) reaction in the intermediate-energy region.

DOI: 10.1103/PhysRevA.96.052701

I. INTRODUCTION

Over the decades, electron-impact ionization processes have been studied extensively over a broad range of projectile energies and kinematic regions, both experimentally and theoretically; for reviews, see Refs. [1,2]. In recent years, there has been considerable interest in complex systems in experiments. In particular, there have been analyses of momentum distributions and the absolute triple differential cross section (TDCS) of energetic electrons in collisions with rare-gas atoms [3–10] due to the rapid developments in measurement techniques in many laboratories [11,12]. Recently, Hargreaves *et al.* [6] reported a detailed experimental measurement of the absolute TDCS of electron-impact ionization of Ne and Ar. This measurement was also compared to calculated results at various levels of theory, i.e., the distorted wave Born approximation (DWBA) augmented with the Gamow factor (DWBA-G) approach [13,14], convergent close-coupling (CCC) [2,5,15], the second-order distorted wave/R-matrix hybrid theory (DW2-RM) [16,17], and the three-body distorted-wave (3DW) approach [18,19]. Comparable agreement between experimental and theoretical results can readily be observed at low energies [e.g., 150 eV for Ne($2p$), 150 eV for Ne($2s$), and 113.5 eV for Ar($3p$)]. However, theoretical predictions deviated noticeably from experimental data in the region of higher energies, e.g., the values were underestimated by a factor of 1.6 and 2.0 at 599.6 eV for Ne ($2p$) and 195 eV for Ar($3p$), respectively. Furthermore, in subsequent (e,$2e$) experiments for Ar($3p$) performed by Ren *et al.* [17] at 195 eV and by Ulu *et al.* [20] at 200 eV, similar disagreement was also observed when comparing theoretical results based on the B-spline R-matrix (BSR) strategy to those measured ones. This illustrates that none of the aforementioned theoretical models can describe correctly the dynamics of electron-impact ionization at relatively high energies, which might be an indication that the applied theoretical models are flawed and must be improved.

Theoretically, the DWBA model is designed to include the long-range direct ionized interaction between the electron projectile and the ionized atomic target, which was shown in several previous works [21,22] to be applicable in high-energy (e,$2e$) reactions, but it fails to predict the magnitude of the absolute TDCS at 599.6 eV, as shown in Ref. [6]. For the BSR model, the short-range higher-order projectile-nucleus interaction is described via the R-matrix method, which yielded impressive agreement with 0–100 eV (e,$2e$) experiments for He [7,9,23], Ne [8,24], and Ar [10,25,26]. It is found nevertheless to yield remarkable discrepancies in the absolute TDCS for e^--Ar($3p$) at 195 eV [17]. In particular, for large-angle scattering the absolute TDCS values were underestimated by a factor of 2–3. One of the key arguments to understand the observed discrepancy might be attributed to the long-range postcollision interaction (PCI), which was crudely neglected in the DWBA model and was partly considered in the BSR model. Within this consideration, the 3DW model that includes the PCI effect via Coulomb factors computed accurately is expected to predict the experiments fairly well within errors. Unfortunately, however, it turned out to yield inconsistent results for the absolute TDCS of the 195 and 200 eV (e,$2e$) reaction of Ar($3p$) [19]. In this context, the discrepancies between theory and experiment are becoming rather elusive, since all the mutual interactions have been actually considered in the theoretical models mentioned above. Inspired by this challenge, it is our aim in this work to seek solutions to this puzzle, and our results predict the experimental TDCS in a more reasonable manner, both in magnitude and angle dependence, as will be presented in the following sections.

We pay particular attention to the Coulomb factor [18] that describes the correlation between two free electrons, which may not suffice to incorporate the largest effect of PCI in the

*xiaoqing-hu@foxmail.com
†wu_yong@iapcm.ac.cn
‡yangwang0624@foxmail.com

three-body system of Ref. [19]. To confirm this speculation, we therefore present a model to analyze the role of PCI for the absolute TDCS of the intermediate-energy $(e,2e)$ reaction. In view of the PCI encoded in the interaction of an incident electron projectile and an ejected electron as the high-order terms, a straightforward treatment is to extend the present DWBA model to high-order components in order to consider the PCI effect more productively. In contrast to the previous work based on the second-order DWBA model (DWBA2), where the contribution of ionization after the excitation process was explicitly analyzed [27,28], we shall point out in the present work that the repulsion after the ionization process can also play a role.

In this work, we neglected the effect of excited states in order to emphasize exclusively the role of PCI, which is considered to be a reasonable assumption for high- and intermediate-energy electron-atom collisions, where ionized cross sections are found to be dominant over excited cross sections by several orders of magnitude. Furthermore, we selected the distorted waves to expand the Green's function, which is more physical than the pseudostates [29] approach. As a first step, we studied the $(e,2e)$ reaction of Ne$(2p)$ using the present DWBA2 model at an impact energy of 599.6 eV. To further verify the developed model, we applied it to explore a more complex atom, i.e., Ar$(3p)$, at 195 eV, for which experimental data are available [30]. Finally, we extended the DWBA model up to the third order (DWBA3) for the purpose of obtaining more accurate results in the Ar$(3p)$ $(e,2e)$ reaction while at the same time examining the high-order influences on the TDCS.

The organization of this article is as follows. The theoretical framework of the DWBA model is presented briefly in Sec. II, where essential formulas are derived and the observables are introduced. In Sec. III, results are discussed in detail and compared to experimental data where available. The conclusion is eventually drawn in Sec. IV. Atomic units are employed throughout the work unless stated otherwise.

II. THEORY

In the $(e,2e)$ reaction, the TDCS is usually given by [31]

$$\frac{d^3\sigma}{d\Omega_f d\Omega_s dE} = (2\pi)^4 \frac{k_f k_s}{k_0} \sum_{av} |T_{fi}|^2, \tag{1}$$

where k_0 is the momentum of the incident electron, and k_f and k_s denote the momentum of the fast and slow electrons, respectively. The subscript av represents a sum over the final and the average over initial magnetic and spin degeneracies. The total transition amplitude can thus be written as

$$T_{fi} = T_{fi}{}^{(1)} + T_{fi}{}^{(2)} + T_{fi}{}^{(3)} + T_{fi}{}^{(4)} + \cdots, \tag{2}$$

where, $T_{fi}^{(j)}$ is the jth-order transition amplitude with $j-1$ Green operators.

In the traditional DWBA model, it is assumed that the total transition amplitude T_{fi} is approximately equal to the first-order transition amplitude, and thus the rest of the high-order terms are all neglected. The Hamiltonian of the collisions system [31] is partitioned as follows:

$$\hat{H} = [(K_1 + U_1) + (K_2 + U_2)] + \frac{1}{|r_1 - r_2|} = \hat{H}_0 + v, \tag{3}$$

where K_1 and K_2 are the kinetic energy operators of electron 1 and electron 2, and U_1 and U_2 are the local, central distorting potential. H_1 and H_2 are the Hamiltonians of electron 1 and electron 2. v refers to the interaction potential between electron 1 and electron 2. The transition amplitude $T_{fi}^{(1)}$ can be written as

$$T_{fi}^{(1)} = \langle \chi^{(-)}(k_s)\chi^{(-)}(k_f)|v|\alpha\chi^{(+)}(k_0)\rangle, \tag{4}$$

where α represents the wave function of the bound state [31]. $\chi^{(+)}(k_0)$, $\chi^{(-)}(k_s)$, and $\chi^{(-)}(k_f)$ are the continuum eigenfunctions of $\hat{H}_0$ with eigenenergy E_0, E_s, and E_f, and they are obtained by solving the single-electron Schrödinger equations

$$(K_{1(2)} + U_{1(2)})|\chi(k)\rangle = E|\chi(k)\rangle. \tag{5}$$

In this paper, in order to emphasize the role of PCI, the polarization potential and exchange potential are not included in the distorting potential. The distorting potentials U [31] are obtained from the target radial orbitals $u_{nl}(r)$, which depend on the electronic configuration of the target,

$$U(r) = \sum_{nl} N_{nl} \int dr' [u_{nl}(r')]^2 / r_>, \tag{6}$$

where $r_>$ is the greater of r and r', and N_{nl} is the number of electrons in each orbital nl. The radial orbitals are obtained with the multiconfiguration Hartree-Fock (MCHF) code [32].

The validation of this model has been demonstrated in a multitude of TDCS calculations [21,22] of high-energy $(e,2e)$ reaction. However, it fails to describe the TDCS quantitatively for intermediate energies, and therefore the high-order transition amplitude may be needed in the calculations to predict the experiments.

In this section, we shall take the second-order term $T_{fi}^{(2)}$ as an example to present our strategy to calculate numerically the high-order transition amplitude. If we consider the continuum distorted wave as expanding functions, one can express $T_{fi}^{(2)}$ as

$$\begin{aligned} T_{fi}^{(2)} &= \lim_{\varepsilon\to 0^+} \langle \chi^{(-)}(k_s)\chi^{(-)}(k_f)|v \frac{1}{E - \hat{H}_0 + i\varepsilon} v|\alpha\chi^{(+)}(k_0)\rangle \\ &= \lim_{\varepsilon\to 0^+} \int \frac{1}{E_0 - E_a - E_b + i\varepsilon} d\vec{k}_a d\vec{k}_b \\ &\quad \times \langle \chi^{(-)}(k_s)\chi^{(-)}(k_f)|v|\chi^{(-)}(k_a)\chi^{(-)}(k_b)\rangle \\ &\quad \times \langle \chi^{(-)}(k_a)\chi^{(-)}(k_b)|v|\alpha\chi^{(+)}(k_0)\rangle, \end{aligned} \tag{7}$$

where $\chi^{(-)}(k_a)$ and $\chi^{(-)}(k_b)$ are also obtained from Eq. (5), and $\vec{k}_a$ and $\vec{k}_a$ correspond to their momenta, respectively. With the relation $d\vec{k} = k^2 dk \sin\theta\, d\theta\, d\varphi$, and integrating k_b from zero to infinity in Eq. (7), we obtain

$$\begin{aligned} T_{fi}^{(2)} &= \lim_{\varepsilon\to 0^+} \int \frac{1}{E_0 - E_a - E_b + i\varepsilon} dk_a dk_b W(k_a, k_b) \\ &= -\pi i \int \frac{1}{\sqrt{2E_0 - k_a{}^2}} W\left(k_a, \sqrt{2E_0 - k_a{}^2}\right) dk_a, \end{aligned} \tag{8}$$

where the integral function $W(k_a,k_b)$ is denoted as

$$W(k_a,k_b) = \int {k_a}^2 {k_b}^2 \sin\theta_a \sin\theta_b d\theta_a d\theta_b d\varphi_a d\varphi_b \times \langle \chi^{(-)}(k_s)\chi^{(-)}(k_f)|v|\chi^{(-)}(k_a)\chi^{(-)}(k_b)\rangle \times \langle \chi^{(-)}(k_a)\chi^{(-)}(k_b)|v|\alpha\chi^{(+)}(k_0)\rangle. \quad (9)$$

We have neglected the principal part [16] of the integral with respect to k_b in Eq. (8), and we shall explain below in more detail the reason why we made this approximation. Usually, the DWBA model describes the $(e,2e)$ reaction as a simple three-body system in which the long-range Coulomb interaction is mainly considered. Due to a large mass ratio of the residual ion to the electron, and long distances between the residual ion and the electrons, the kinetic energy of the residual ion is negligible. Similarly, for the present high-order Born approximation models, the PCI emphasized in these models also belongs to the long-range interaction, and we can thus suppose that the total energy of the incident electron and the ejected electron is conservative. Hence for the integral of the Green's function, the contribution of singularity is the most important; it corresponds to the complex part of the integral result, as seen in Eq. (8).

For the present second-order DWBA model, the interaction with which we are most concerned, namely the scattering potential v, can be divided into two parts by the expansion of the Green's function using the continuum distorted wave. One is the direct ionization interaction, which directly promotes the electron from the bound state to the continuum state. The other is the postcollision interaction (PCI), which represents the repulsion of two outgoing electrons. The second-order physical process corresponds with the fact that the bound electron is first ionized directly into the continuum state and then evolves into the final state because of the influence of PCI.

To calculate the transition amplitude numerically, we expand the distorted functions into a partial wave form, and we formulate the direct ionization amplitude [31] as

$$\langle \chi^{(-)}(k_a)\chi^{(-)}(k_b)|v|\alpha\chi^{(+)}(k_0)\rangle = \frac{(4\pi)^{5/2}}{(2\pi)^{9/2}}(k_0k_ak_b)^{(-1)} \sum_{L_aL_bL_0}\sum_{M_a\lambda} \begin{pmatrix} L_0 & \lambda & L_a \\ 0 & 0 & 0 \end{pmatrix}\begin{pmatrix} L_0 & \lambda & L_a \\ 0 & -M_a & M_a \end{pmatrix} \times \begin{pmatrix} l & \lambda & L_b \\ 0 & 0 & 0 \end{pmatrix}\begin{pmatrix} l & \lambda & L_b \\ m & -M_a & M_a - m \end{pmatrix} R^{(\lambda)}_{L_aL_bL_0l}(k_a,k_b,k_0)Y^*_{L_b(M_a-m)}(\hat{k}_b)Y_{L_aM_a}(\hat{k}_a). \quad (10)$$

Similarly, the PCI amplitude can be written as

$$\langle \chi^{(-)}(k_s)\chi^{(-)}(k_f)|v|\chi^{(-)}(k_a)\chi^{(-)}(k_b)\rangle = \frac{(4\pi)^4}{(2\pi)^{(6)}}\frac{1}{(k_ak_bk_sk_f)} \sum_{L_aL_bL_sL_f}\sum_{M_aM_bM_f\gamma} \begin{pmatrix} L_a & \gamma & L_f \\ 0 & 0 & 0 \end{pmatrix}\begin{pmatrix} L_a & \gamma & L_f \\ M_a & -M_f - M_a & M_f \end{pmatrix}\begin{pmatrix} L_b & \gamma & L_s \\ 0 & 0 & 0 \end{pmatrix} \times \begin{pmatrix} L_b & \gamma & \mathrm{L_s} \\ M_b & -M_f - M_a & M_f + M_a - M_b \end{pmatrix} R^{(\gamma)}_{L_aL_bL_sL_f}(k_ak_bk_sk_f)Y_{L_aM_a}(\hat{k}_a)Y^*_{L_bM_b}(\hat{k}_b)Y^*_{L_s(M_f+M_a-M_b)}(\hat{k}_s)Y_{L_fM_f}(\hat{k}_f). \quad (11)$$

The multipolar expansion [31] of v used in Eqs. (10) and (11) is

$$v(r_1,r_2) = \sum_{\lambda\mu} 4\pi\hat{\lambda}^{-2}\frac{r_<^\lambda}{r_>^{\lambda+1}}Y_{\lambda\mu}(\hat{r}_1)Y^*_{\lambda\mu}(\hat{r}_2), \quad (12)$$

where $r_<$ and $r_>$ denote the lesser and greater, respectively, of r_l and r_2. The factor γ in Eq. (11) represents the change of angular momentum number and can thus reflect the strength of PCI.

The terms of the radial operators $R^{(\lambda)}_{L_aL_bL_0l}(k_a,k_b,k_0)$ and $R^{(\gamma)}_{L_aL_bL_sL_f}(k_ak_bk_sk_f)$ are defined as follows:

$$R^{(\lambda)}_{L_aL_bL_0l}(k_a,k_b,k_0) = i^{L_0-L_a-L_b}\exp[i(\sigma_{L_0}+\sigma_{L_a}+\sigma_{L_b})]\hat{l}\hat{L}_0^2\hat{L}_a\hat{L}_b \times \int dr_1 \int dr_2 u_{L_a}(k_a,r_1)u_{L_b}(k_b,r_2)v_\lambda(r_1,r_2)u_{nl}(r_2)u_{L_0}(k_0,r_1), \quad (13)$$

$$R^{(\lambda)}_{L_aL_bL_sL_f}(k_a,k_b,k_s,k_f) = i^{L_a+L_b-L_s-L_f}\exp[i(\sigma_{L_a}+\sigma_{L_b}-\sigma_{L_s}-\sigma_{L_f})] \times \hat{L}_s\hat{L}_f\hat{L}_a\hat{L}_b \int dr_1 \int dr_2 u_{L_f}(k_f,r_1)u_{L_s}(k_s,r_2)v_\lambda(r_1,r_2)u_{L_a}(k_a,r_1)u_{L_b}(k_b,r_2). \quad (14)$$

Since the scattering potential v only works for the radial operators $R^{(\lambda)}_{L_aL_bL_0l}(k_a,k_b,k_0)$ and $R^{(\gamma)}_{L_aL_bL_sL_f}(k_ak_bk_sk_f)$, we can use the spherical harmonics orthogonal relationship [see Eq. (15)] to integrate $\hat{k}_a$ and $\hat{k}_b$ in Eq. (11). This integral not only simplifies the calculation of the high-order transition amplitude, but it also ensures the conservation of total magnetic quantum numbers, i.e., $\alpha\chi^{(+)}(k_0) = \chi^{(-)}(k_a)\chi^{(-)}(k_b) = \chi^{(-)}(k_s)\chi^{(-)}(k_f)$, which is the necessary requirement for the $(e,2e)$ reaction,

$$\int_0^{2\pi}\int_0^{\pi} Y^*_{l_1m_1}(\theta,\varphi)Y_{l_2m_2}(\theta,\varphi)\sin\theta\, d\theta\, d\varphi = \delta_{l_1l_2}\delta_{m_1m_2}. \quad (15)$$

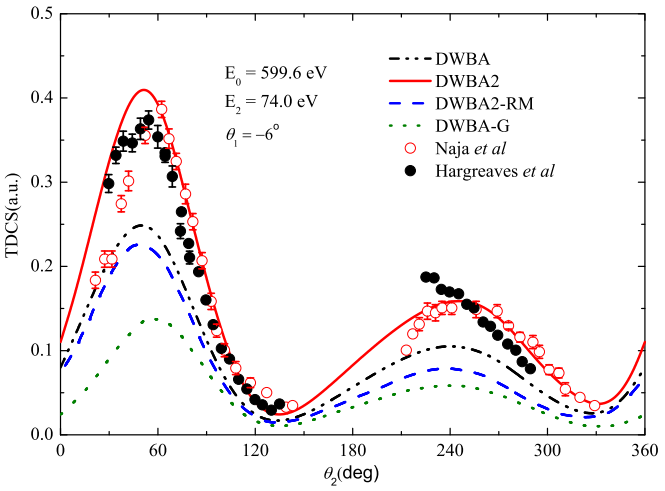

FIG. 1. Absolute TDCS of Ne($2p$) as a function of ejected angle (θ_2) in the coplanar asymmetric geometry. Solid circles: experimental data of Hargreaves *et al.* [6]; open circles: experimental data of Naja *et al.* [13], after normalizing in the binary peak; solid curve: present DWBA2 calculation; dashed curve: DWBA2-RM calculation [6]; dotted curve: DWBA-G calculation [6]; dashed-dotted curve: present DWBA calculation. The relevant parameters are indicated in the legend.

Several key points are summarized as follows for the numerical calculation of the formula (9), and they clearly show the physical mechanism reflected by the second-order Born approximation. (i) The energies of outgoing electrons determine the integral range of the electron momentum k_a through the PCI amplitude [Eq. (11)], which converges in a small vicinity of the fast electron momentum k_f for the high- and intermediate-energy $(e,2e)$ reaction. Meanwhile, in this integration region, the direct ionization amplitude [Eq. (10)] is essentially unchanged and is equal to the ionization amplitude of the DWBA. (ii) The PCI amplitude changes the partial waves population of the direct ionization amplitude. Upon increasing the PCI strength γ, the shape of the cross section changes significantly. (iii) In the present calculations, the maximum value of γ is set to 2, which means the PCI is weak at high and intermediate energies. It should be noted that the present high-order model considers the direct ionization interaction and PCI effects simultaneously. However, only the PCI affects the convergence of the high-order Born approximation.

III. RESULTS AND DISCUSSION

In this work, the absolute TDCS for the $(e,2e)$ reaction of Ne($2p$) at an impact energy of 599.6 eV was calculated using the present DWBA2 model with a slow electron energy of $E_2 = 74$ eV. Our results are presented in Fig. 1, along with experimental data [6,13] and other theoretical results [6], as a function of the ejected electron angle (θ_2). The scattering angle θ_1 was set to -6° (experimental condition) so that the comparison could be performed on an equal footing. Clearly, calculated TDCS results with the present DWBA2 model are in nice agreement with available experimental cross sections measured by Hargreaves *et al.* [6], both in the magnitude as well as the dependence of the scattering angle, which improves the quality of theoretical predictions significantly when comparing to other DWBA models based on distinct approximations. More precisely, the conventional DWBA model (dashed-dotted curve) underestimated the magnitude of the absolute TDCS by nearly a factor of 1.5, especially in the vicinity of 60° and 240°. In addition, the DWBA-G model underestimated the magnitude of absolute TDCS by a factor of $\sim$1.8 in the considered angle range, although the DWBA-G model also considers the role of PCI within an approximate Coulomb factor, i.e., the Gamow factor. The significant improvement of the present results may be attributed to the different treatments of PCI, implying that the present DWBA2 model indeed incorporates more PCI effects than the Gamow factor.

On the other hand, the DWBA2-RM model is also used for comparison. Quantitatively, the magnitudes predicted by the DWBA2-RM model are quite similar to those predicted by the DWBA model, and the difference is estimated to be less than 3%. It should be noted that the short-range higher-order projectile-nucleus interaction is considered more accurate through the R matrix in the DWBA2-RM model than by distorted potentials in the DWBA. As a consequence, short-range interactions play only a marginal role in the intermediate-energy $(e,2e)$ reaction, which is not as important as the role of PCI in the case shown in Fig. 1.

With respect to the overall shape of the TDCS, i.e., the dependence of the TDCS on the scattering angle, all of the four theoretical models result in the same shape as that depicted in experiments, characterized by a sequence of extrema in the considered range (maxima at around 60° and 240° and minima around 130° and 330°). This is not totally surprising, since the shape of the TDCS is dominated by the wave function of Ne($2p$). In the present DWBA2 calculations, the strength factor γ of PCI is summarized from 0 to 1 which already suffices to yield the converged results. Hence, the low-order PCI is the crucial factor to determine the magnitude of the absolute TDCS for the intermediate energy $(e,2e)$ reaction.

To further verify the present model and confirm the role of PCI, we also calculated the absolute TDCS for single ionization of the Ar($3p$) ground state with an incident electron energy of $E_0 = 195$ eV, a slow electron energy of $E_2 = 10$ and 15 eV, and a scattering angle θ_1 ranging from -5° to -20° separated by 5°. For these calculations, we used in DWBA2 the maximum value of the PCI strength factor, i.e., $\gamma = 2$. The results are depicted in Figs. 2–4 as a function of the ejected angle (θ_2) in three planes (xy, xz, and yz) within the laboratory frame. For comparison, experimental data measured by Ren *et al.* [17] are also shown together with other calculations of DWBA2-RM [17] and BSR-482 [25]. By analyzing the TDCS in three planes, it is expected that the relationship between PCI and the ejected angle will be revealed.

Figure 2 presents the absolute TDCS calculated using the present DWBA2 and DWBA3 models in the perpendicular plane xy. The present high-order calculations show similar structures in the relative shape of the TDCS compared with the standard DWBA calculation, but the magnitude of the cross section has been roughly enhanced by a factor of 2–3. This can occur because the PCI effect remains unchanged in the xy plane when the ejected angle varies from 0° to 360°.

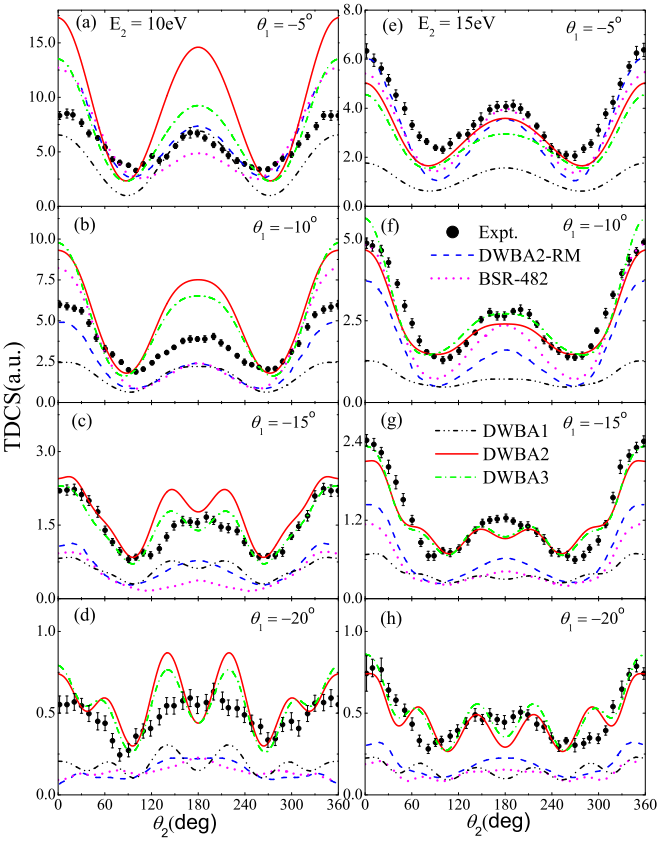

FIG. 2. Absolute TDCS of Ar(3p) as a function of ejected angle (θ_2) at an impact energy $E_0 = 195$ eV in the xy plane. Parts (a)–(d) are for $E_2 = 10$ eV (left panel), and parts (e)–(h) are for $E_2 = 15$ eV (right panel). The measured scattering angle varies from -5° (top panel) to -20° (bottom panel) in a step of 5°. Solid circles: experimental data of Ren *et al.* [30]; solid curve: present DWBA2 calculation; dashed-dotted curve: present DWBA3 calculation; dashed and dense dots curve: standard DWBA calculation; dashed curve: DWBA2-RM calculation [30]; dotted curve: BSR calculation [25].

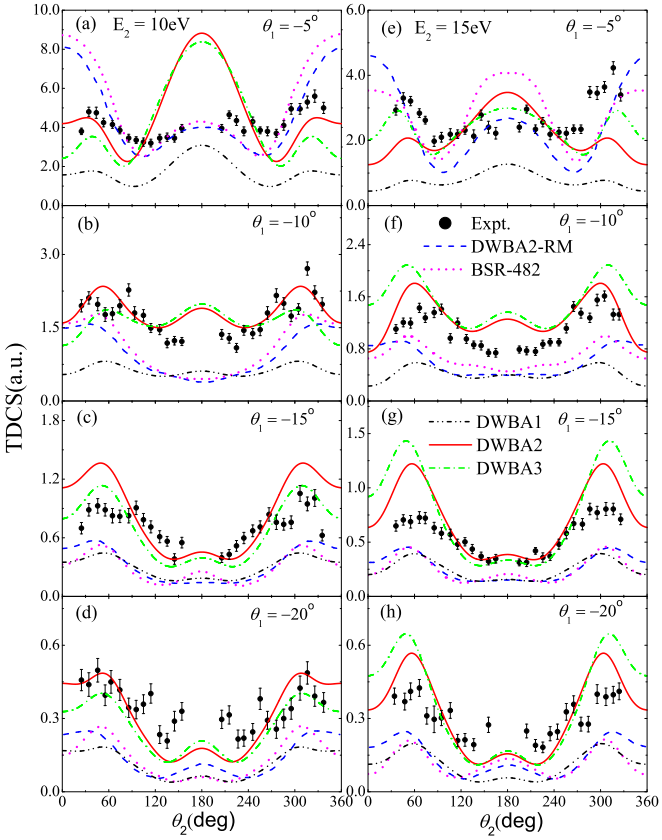

FIG. 3. Same as Fig. 2, but the slow electron is detected in the xz plane.

Figure 3 reports a similar set of results to those shown in Fig. 2, but in another perpendicular plane, i.e., the xz plane. In contrast to the xy plane, with the ejected angle θ_2 changing from 180° to 0° or to 360°, the angle between the two outgoing electrons decreases rapidly. In this sense, the PCI varies sensitively with respect to different ejected angles. This is also supported by comparing the present DWBA3 results with those from DWBA2, from which we find a pronounced difference at the ejected angle $0^\circ < \theta_2 < 90^\circ$ and $270^\circ < \theta_2 < 360^\circ$; the difference in the convergence indicates the change of PCI. Figure 4 presents the absolute TDCS calculated using the present high-order DWBA models in coplanar asymmetric geometry (the yz plane). In this plane, the dependence of shape on the ejected angle is more obvious.

For clarity, two aspects are worth pointing out in some detail: (i) The calculations based on DWBA3, which take into account the high-order PCI effect, have more obvious influences on the shape of the TDCS than those based on DWBA2 with the low-order PCI effect. Actually, it depends on the ratio of the direct ionized interaction to the PCI, which determines the role of PCI in a different order Born approximation. (ii) The shape dependence on the ejected angle for $E_2 = 10$ eV differs from that for 15 eV. As can be seen in Figs. 3(a)–3(d), 3(e) and 3(f), when taking the DWBA2 results for comparison, the prediction by the DWBA3 model increases the TDCS in Figs. 3(a)–3(d) and decreases it in Figs. 3(e) and 3(f) when the angle between two outgoing electrons becomes large, i.e., $0^\circ < \theta_2 < 90^\circ$ and $270^\circ < \theta_2 < 360^\circ$.

By comparing all theoretical results with experimental data, it is found that our present calculations yield more satisfactory agreement with experimental results for the magnitude of the TDCS than other methods, especially in the large-angle scattering region. Concerning the shape of the TDCS, relatively good agreement can also be found in the xy and xz planes. This illustrates that the PCI plays the more important role in out-of-plane geometries. However, in the yz plane, it is seen that the BSR results agree fairly well with experiments in the full measured energies and angles. The reason for this agreement may be that the high-order projectile-nucleus interactions play a more important role in this plane.

Figure 5 compares results obtained using the three-body distorted wave (3DW) approach with those obtained using the present high-order DWBA model for the Ar(3p) (e,2e) reaction. Also note that the 3DW approach includes the role of PCI by calculating the Coulomb factor accurately. As seen in Fig. 5, a better agreement with experimental measurement can be found in the present predictions for the magnitude of the TDCS. In fact, the 3DW predictions [19] did not improve too much on top of the standard DWBA model. Therefore,

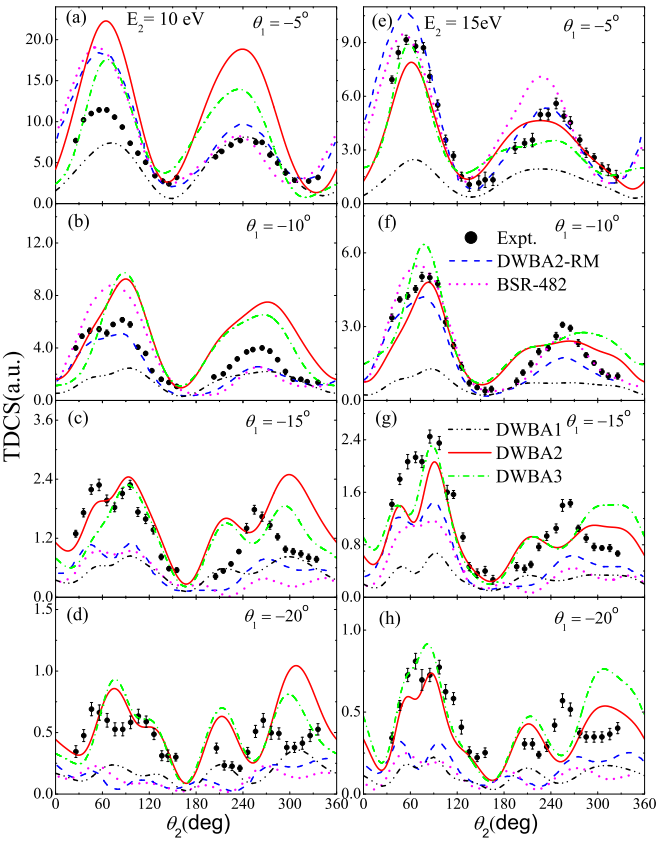

FIG. 4. Same as Fig. 2, but the slow electron is detected in the yz plane.

we conclude that the Coulomb factor alone may not suffice to contain the largest effect of PCI quantitatively in the three-body system; instead, one must treat explicitly the high-order transition amplitude.

IV. SUMMARY AND CONCLUSIONS

In conclusion, we have presented in this paper a high-order DWBA model with the continuum distorted-waves expansion, which considers the postcollision interaction (PCI) accurately. Then we applied it to calculate the absolute triple differential cross section for single ionization of Ne($2p$) by 599.6 eV and Ar($3p$) by 195 eV. Comparing with the standard DWBA calculation, the present high-order calculations show similar structure in the relative shape of the TDCS, but the magnitude of the cross section has been significantly improved to reproduce well the experimental results. Quantitatively, the present results are estimated to be a factor of 1.6 for Ne and 2–3 for Ar in comparison with those obtained by the standard DWBA approach. Compared with other theoretical predictions, an

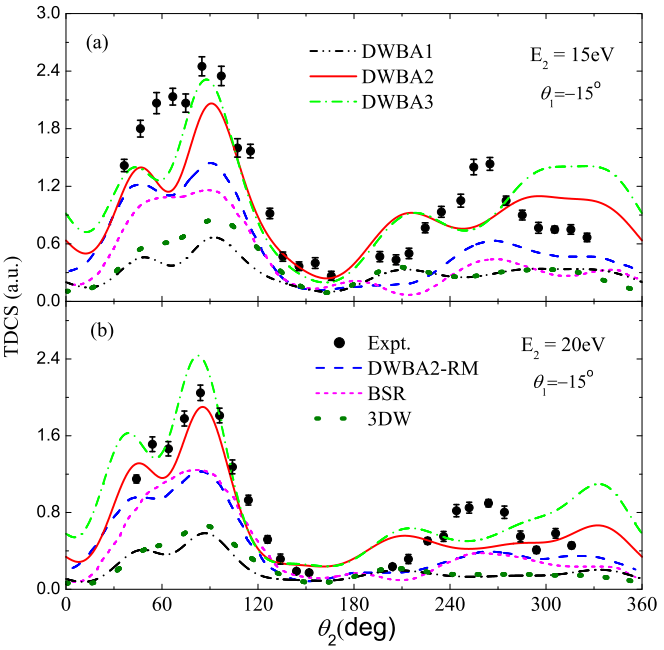

FIG. 5. Same as Fig. 4, but the olive dotted line represents the 3DW calculations [19].

overall agreement with the experiments in many cases is found to be better if the PCI is properly considered within the high-order model, indicating the important role of the PCI in the electron-impact ionization process. Furthermore, comparing the results of DWBA2 and DWBA3 with the experiment data, a conclusion can be drawn that the effect of PCI on the shape of the TDCS is the high-order part of the PCI effect, and the effect on the magnitude of the TDCS is more important for the intermediate-energy (e,$2e$) reaction.

The satisfactory agreement between the present results and the experimental data confirms our arguments that the Coulomb factor that accounts for the correlation between two free electrons is not enough to describe the largest effect of PCI in the three-body system. In addition, this work reveals that it is possible to use the fully perturbative high-order DWBA model to obtain the accurate absolute TDCS for the low-energy (e,$2e$) reaction of a complex atom as long as the short-range higher-order projectile-nucleus interaction is considered reasonably in the near future.

ACKNOWLEDGMENTS

This work was supported by the National Key Research and Development Program of China (Grant No. 2017YFA0402300), the Science Challenge Project (Grant No. TZ2016005), and the National Natural Science Foundation of China (Grants No. 11534011, No. 11774030, No. 11404081, and No. 11504421).

[1] I. E. McCarthy and E. Weigold, Rep. Prog. Phys. **54**, 789 (1991).
[2] I. Bray, D. V. Fursa, A. S. Kadyrov, A. T. Stelbovics, A. S. Kheifets, and A. M. Mukhamedzhanov, Phys. Rep. **520**, 135 (2012).
[3] T. N. Rescigno, Science **286**, 2474 (1999).
[4] S. Bellm, J. Lower, E. Weigold, I. Bray, D. V. Fursa, K. Bartschat, A. L. Harris, and D. H. Madison, Phys. Rev. A **78**, 032710 (2008).

[5] I. Bray, D. V. Fursa, A. S. Kadyrov, and A. T. Stelbovics, Phys. Rev. A **81**, 062704 (2010).
[6] L. R. Hargreaves, M. A. Stevenson, and B. Lohmann, J. Phys. B **43**, 205202 (2010).
[7] O. Zatsarinny and K. Bartschat, Phys. Phys. Lett. **107**, 023203 (2011).
[8] T. Pflüger, O. Zatsarinny, K. Bartschat, A. Senftleben, X. Ren, J. Ullrich, and A. Dorn, Phys. Rev. Lett. **110**, 153202 (2013).
[9] X. Ren, A. Senftleben, T. Pflüger, K. Bartschat, O. Zatsarinny, J. Berakdar, J. Colgan, M. S. Pindzola, I. Bray, D. V. Fursa *et al.*, Phys. Rev. A **92**, 052707 (2015).
[10] X. Ren, S. Amami, O. Zatsarinny, T. Pflüger, M. Weyland, A. Dorn, D. Madison, and K. Bartschat, Phys. Rev. A **93**, 062704 (2016).
[11] M. Takahashi, T. Saito, M. Matsuo, and Y. Udagawa, Rev. Sci. Instrum. **73**, 2242 (2002).
[12] J. Ullrich, R. Moshammer, A. Dorn, R. Dörner, L. Ph. H. Schmidt, and H. Schmidt-Böcking, Rep. Prog. Phys. **66**, 1463 (2003).
[13] A. Naja, E. M. Staicu Casagrande, A. Lahmam-Bennani, M. Stevenson, B. Lohmann, C. Dal Cappello, K. Bartschat, A. Kheifets, I. Bray, and D. V. Fursa, J. Phys. B **41**, 085205 (2008).
[14] A. S. Kheifets, A. Naja, E. M. S. Casagrande, and A. Lahmam-Bennani, J. Phys. B **41**, 145201 (2008).
[15] S. Jones and D. H. Madison, Phys. Rev. A **62**, 042701 (2000).
[16] R. H. G. Reid, K. Bartschat, and A. Raeker, J. Phys. B **31**, 563 (1998).
[17] X. Ren, I. Bray, D. V. Fursa, J. Colgan, M. S. Pindzola, T. Pflüger, A. Senftleben, S. Xu, A. Dorn, and J. Ullrich, Phys. Rev. A **83**, 052711 (2011).
[18] D. H. Madison and O. Al-Hagan, J. At. Mol. Opt. Phys. **2010**, 367180 (2010).
[19] S. Amami, M. Ulu, Z. N. Ozer, M. Yavuz, S. Kazgoz, M. Dogan, O. Zatsarinny, K. Bartschat, and D. Madison, Phys. Rev. A **90**, 012704 (2014).
[20] M. Ulu, Z. N. Ozer, M. Yavuz, O. Zatsarinny, K. Bartschat, M. Dogan, and A. Crowe, J. Phys. B **46**, 115204 (2013).
[21] S. Rioual, B. Rouvellou, A. Pochat, J. Rasch, H. R. J. Walters, C. T. Whelan, and R. J. Allan, J. Phys. B **30**, L475 (1997).
[22] A. Prideaux and D. H. Madison, Phys. Rev. A **67**, 052710 (2003).
[23] O. Zatsarinny and K. Bartschat, Phys. Rev. A **85**, 062709 (2012).
[24] O. Zatsarinny and K. Bartschat, Phys. Rev. A **86**, 022717 (2012).
[25] O. Zatsarinny and K. Bartschat, Phys. Rev. A **85**, 032708 (2012).
[26] X. Ren, T. Pflüger, J. Ullrich, O. Zatsarinny, K. Bartschat, D. H. Madison, and A. Dorn, Phys. Rev. A **85**, 032702 (2012).
[27] P. J. Marchalant, C. T. Whelan, and H. R. J. Walters, J. Phys. B **31**, 1141 (1998).
[28] Y.-Z. Zhang, Y. Wang, and Y.-J. Zhou, Chin. Phys. B **23**, 063402 (2014).
[29] C. D. Cappello, B. Hmouda, A. Naja, and G. Gasaneo, J. Phys. B **46**, 145203 (2013).
[30] X. Ren, A. Senftleben, T. Pflüger, A. Dorn, K. Bartschat, and J. Ullrich, Phys. Rev. A **83**, 052714 (2011).
[31] I. E. McCarthy, Aust. J. Phys. **48**, 1 (1995).
[32] C. F. Fischer, T. Brage, and P. Jönsson, *Computational Atomic Structure: An MCHF Approach* (Institute of Physics, Bristol, 1997).